Next Materials 9 (2025) 101279

Contents lists available at ScienceDirect

Next Materials

journal homepage: www.sciencedirect.com/journal/next-materials

Comprehensive characterization of sustainably synthesized lignin-based polyols towards thermoset materials

Bram Jacobs [a,b], Geert-Jan Graulus [b], Katrien V. Bernaerts [c], An Verberckmoes [a,*]

[a] Faculty of Engineering and Architecture, Department of Materials, Textiles and Chemical Engineering, Industrial Catalysis and Adsorption Technology (INCAT), Ghent University, Valentin Vaerwyckweg 1, Ghent 9000, Belgium
[b] Hasselt University, Institute for Materials Research (imo-imomec), Biomolecule Design Group, Agoralaan (Building D), Diepenbeek 3590, Belgium
[c] Sustainable Polymer Synthesis Group, Aachen-Maastricht Institute for Biobased Materials (AMIBM), Faculty of Science and Engineering, Maastricht University, Urmonderbaan 22, Geleen, 6167 RD, the Netherlands

ARTICLE INFO

Keywords:
Organosolv lignin
Ethylene carbonate
Glycerol carbonate
^{13}C NMR
^{31}P NMR

ABSTRACT

Lignin, the most abundant aromatic biopolymer, has a high potential as an alternative to fossil resources in the chemical industry, especially within thermoset materials not only as a filler material but as reactant contributing to product properties. However, incorporating lignin is challenging because of the low and non-uniform reactivity of the functional groups and lack of characterization understanding. This study evaluated both ethylene carbonate and glycerol carbonate to obtain a polyol with solely aliphatic OH functionalities by modifying four different organosolv lignins from beech and poplar. The modification with ethylene carbonate yielded a polyol with aliphatic OH content in agreement with the theoretically calculated aliphatic OH content by conversion of native aliphatic and phenolic OH functionalities and COOH moieties. The modification with glycerol carbonate resulted in a more complex product with a lower aliphatic OH content than expected. This bias is caused by (1) non-reactivity of native alOH moieties with glycerol carbonate and (2) the formation of cyclic CO_3 moieties on top of lignin. The hypothesis regarding loss of low molecular weight fragments in the work up was refuted. In addition to ^{31}P NMR as a widely used analysis, ^{13}C NMR was applied throughout the study and was successfully used in the aliphatic OH content determination in OL feedstocks as well as contributing to glycerol carbonate modified lignin with direct quantification of the 1,2-diol content and cyclic CO_3 content. The uniform and improved reactivity towards thermoset development was demonstrated by an esterification with propionic acid as a proof-of-concept for *e.g.* polyester development

1. Introduction

Lignin, the second most abundant biomacromolecule, is currently being incinerated to produce low-value energy [1–3]. However, many studies report the depolymerization as a strategy – to avoid merely incineration – to obtain biofuels and valuable aromatic compounds such as vanillin. A recent perspective by Slabon *et al.* questions if the selective depolymerization of lignin is not merely an endless quest and criticizes the predominance of lignin in combustion processes which inherently competes and suppresses the application possibilities as a valuable biomacromolecule [1]. Instead of changing the macromolecular structure of lignin, modification strategies – such as phenolation and etherification – can enhance the reactivity of the macromolecular lignin into a functional polymer in a wide variety of applications such as phenol-formaldehyde resins, polyesters and polyurethanes [4–10].

A well-known modification strategy to obtain a polyol is the etherification of OH functionalities into aliphatic OH (alOH) moieties [4,11,12]. From a historical perspective, epoxides such as cyclic ethylene and propylene oxide and epichlorohydrine are among the most popular modifying reagents [4,7,9,13]. Keck *et al.* modified wheat straw soda lignin with KOH (0.2 eq.) and propylene oxide (10 eq.) for 16 h at 100 °C in order to obtain alOH moieties. Afterwards, they further modified the lignin with methacryloyl chloride to obtain a liquid, light-induced curable, 3D-printable lignin-based resin [14]. Passauer *et al.* cross-linked pine Kraft lignin, spruce organosolv lignin and beech organosolv lignin with poly(ethylene glycol) diglycidyl ether (PEGDE) in 3.3 M NaOH (aq.) resulting in water-swellable hydrogels [15–17]. Lee *et al.* oxypropylated methanol-insoluble Kraft lignin (from softwood) with

* Corresponding author.
E-mail address: An.Verberckmoes@ugent.be (A. Verberckmoes).

https://doi.org/10.1016/j.nxmate.2025.101279
Received 31 July 2025; Received in revised form 17 September 2025; Accepted 28 September 2025
Available online 1 October 2025

propylene oxide (≥ 20 eq.) in the presence of NaOH at 40 °C for 12 h (under reflux). The methanol-insoluble fraction was characterized as a high molecular weight residue with a high hydroxyl number whereby the solubility in organic solvents was low because of a high T_g (ideal for good thermal resistance). After oxypropylation, a bio-polyester was developed with sebacic acid in 1,4-dioxane with H_2SO_4 as a catalyst at 100 °C for 12 h, and afterwards cured at 120 °C under vacuum. Finally, the bio-polyester has a good thermal stability with the aid of the oxypropylated Kraft lignin [5]. Besides several unwanted products such as polypropylene oxide, these epoxide reagents are acutely toxic and carcinogenic as a flammable gas (= ethylene oxide) or volatile liquid (= propylene oxide) and potentially prone to self-polymerization when heated [5–7]. Thus, merely using lignin is not a sustainable approach for future chemistry as green processes involve more than solely bio-based compounds (e.g. critical elements, additional solvents, batch/continuous…) [7,11].

Cyclic carbonates fill in the existing gap between etherifying agents and safe and sustainable chemicals with high boiling points, lower risk involvement and potentially more sustainable synthesis pathways. Moreover, the oxyalkylation reaction of beech OL with $GlyCO_3$ (and limited $EtCO_3$ reactant at 150 °C) was evaluated in depth in a previous study by Jacobs *et al.* with key findings such as – but not limited to – complete conversion of phenolic OH (phOH) and COOH functionalities and a temperature at 175 °C which is high enough to minimize the formation of undesired cyclic CO_3 while sufficiently suppressing homopolymerization of $GlyCO_3$ in order to successfully incorporate the modified lignin in self-healing boronate ester gels [11]. In order to obtain 1,2-diols, the cyclic CO_3 groups are an unwanted product yet these functional groups can advantageously be used in *e.g.* non-isocyanate polyurethanes by aminolysis of cyclic carbonates, but this approach is not further discussed in this contribution [7,13,18]. Xuefeng *et al.* used a mixture of PEG400 as viscosity modifier and $EtCO_3$ as reactant in different mass ratios (with small amounts of H_2O to convert excess $EtCO_3$ into ethylene glycol) together with K_2CO_3 to modify a softwood Kraft lignin at 140 – 170 °C for 10 – 30 min. Afterwards, the bio-polyol was mixed with a Sn-catalyst, silicon oil surfactant, neutralizer (H_2SO_4) and blowing agent (H_2O) and foaming occurred after a polyisocyanate mixture was added resulting in a promising route towards more green rigid polyurethane foams [6]. Wang *et al.* fractionated a biorefinery lignin with bio-ethanol (M_W homogenization) followed by modification via ethoxylation (OH functionality homogenization) with $EtCO_3$ at 130 °C and Na_2CO_3 catalyst for 30 – 60 mins. The lignin product was then further used in corrosion-resistant PUR coating development with hexamethylene diisocyanate. The results show improved corrosion resistance compared to merely adding non-pretreated lignin in the synthesis [19]. Dunne *et al.* oxyalkylated lignin (from wheat straw, softwood and a hardwood obtained via resp. organosolv, Kraft and hydrolysis) with $PrCO_3$ and DBU as catalyst at 150 °C for 90 mins in a 2 L benchtop Parr reactor with periodical pressure release to avoid buildup of CO_2. Replacing 10 – 30 wt % of fossil-based polyol with reactive liquid modified lignin resulted in flexible foams with higher elastic moduli and lower tensile strength and lower elongation. The densities of the foams were – in general – higher because of higher hydroxyl content and therefore faster curing rates resulting in limited time for gas bubbles to expand. Residual $PrCO_3$ lowered the thermal stability and glass transition temperature of the foams. In conclusion, a 20 wt% substitution with a high molecular weight, modified Kraft lignin met the automotive seating manufacturing criteria with a 5.3 % reduction in isocyanate addition to improve flexibility [10].

While modifying the OH functionalities of lignin is a viable strategy, the use of cyclic carbonates is still growing. In this work, different organosolv lignins (purchased or in-house extracted from beech and poplar biomass) were evaluated in the oxyalkylation with ethylene carbonate ($EtCO_3$) and glycerol carbonate ($GlyCO_3$) to obtain lignin-based polyols with uniform functionality and high alOH contents. An overview of the reactions and side-reactions for both cyclic carbonates with alOH and phOH moieties are illustrated in Figure S1. Experimentally obtained results were evaluated with theoretically calculated values with regard to the (expected) OH content upon oxyalkylation and formula optimization was performed to determine the 1,2-diol content after oxyalkylation with $GlyCO_3$. Furthermore, ^{13}C NMR was applied as a characterization technique to directly quantify the 1,2-diol groups and (unwanted) cyclic CO_3 moieties together with a discussion regarding the benefits and hurdles of ^{13}C NMR over ^{31}P NMR. Wherever necessary, complementary techniques were used such as Attached Proton Test (APT)-^{13}C NMR and 1H-13C HSQC NMR to identify certain NMR signals. Finally, a green and direct esterification was applied to the OL feedstocks as well as to the modified feedstocks to evaluate the reactivity of the newly formed (and native) alOH functionalities over phOH moieties. These esterified lignins can then further be applied in – but not limited to – analytical purposes as a mean to analyze the lignin structure (*e.g.* SEC with tetrahydrofuran) or as a green additive with plasticizing effect and a high compatibility with other polymer blends [20,21].

2. Materials and methods

2.1. Chemicals

All lignins used in this study were obtained via an organosolv extraction of hardwood biomass. OL_1 and OL_2 were obtained from Fraunhofer CBP by an organosolv process of beech wood. The OL_3 and OL_4 feedstocks were in-house produced from poplar wood by a laboratory-scale organosolv extraction procedure [22]. Prior to any experiment and analysis, the OL feedstocks were milled to a powder by an electric grinder and subsequently dried for 4 h at 60 °C.

Deuterated chloroform ($CDCl_3$) stabilized with silver foil and deuterated dimethyl sulfoxide (DMSO-d_6) were purchased from Eurisotop. Dimethyl sulfoxide (DMSO, HPLC grade, 99.9 +%) was bought from Biosolve. Acetone (99 +%), ethyl acetate (>99.8 %), hydrochloric acid (HCl, 37 %), tetrahydrofuran (THF, 99.8 +%), potassium carbonate (K_2CO_3, 99 +%) and potassium hydroxide (KOH) pellets were purchased from Chem-Lab. 2-chloro-4,4,5,5-tetramethyl-1,3,2-dioxaphospholane (TMDP, 95 %), anhydrous pyridine (99.8 %), chromium(III)acetylacetonate ($Cr(acac)_3$, 97 %), lithium bromide (LiBr, ≥99 %), *endo*-N-hydroxy-5-norbornene-2,3-dicarboxylic acid imide (NHND, 97 %), benzene-1,4-diboronic acid (≥95.0 %) and 1,3,5-trioxane (≥99 %) were purchased from Sigma-Aldrich. Propionic acid (≥99.5 %) was purchased from Carl Roth. Ethylene carbonate ($EtCO_3$, >99.0 %) and glycerol carbonate ($GlyCO_3$, >90.0 %) were purchased from TCI Europe.

2.2. Oxyalkylation of OL feedstocks

A two-neck round-bottom flask (25 mL) was filled with ± 0.50 g lignin and 0.1 equivalents K_2CO_3 (with respect to the total OH content of OL). Subsequently, an excess of either ethylene carbonate ($EtCO_3$) or glycerol carbonate ($GlyCO_3$) (10 equivalents relative to the total OH content = sum of alOH, phOH and COOH functionalities) was transferred into the flask. Next, both necks were closed with rubber septa and the flask was flushed with N_2 for 1 min. A needle connected to a balloon filled with N_2 was placed through the septum to counter the pressure build-up by CO_2 release during the reaction. The flask was then immersed in a pre-heated oil bath at 150 °C (for $EtCO_3$) or at 175 °C (for $GlyCO_3$). After a two-minute pre-heat time (at the corresponding reaction temperature) at 800 rpm stirring speed, the stirring speed was set to 1600 rpm. After reaction, the flask was removed from the oil bath and the reaction medium was precipitated, while still being hot, in a 200 mL HCl (0.01 mol L^{-1}) solution (with high stirring speed which created a visible vortex). The solution was stirred for another 30 min before filtering with a Buchner filter (Whatman grade 1) to avoid/minimize trapped cyclic carbonates and poly($GlyCO_3$) in the precipitate. The solid lignin was scraped from the filter and transferred to a Petri dish and

further dried in a drying oven (VWR) at 60 °C prior to analysis.

2.3. Hydrolysis of the cyclic CO_3 moieties

Around 100 mg of modified lignin with $GlyCO_3$ was first dried and then transferred to a round-bottom flask (50 mL) together with 5 mL of a 0.2 mol L^{-1} KOH solution in ethanol. Hydrolysis was performed for 15 min under reflux in an oil bath. After reaction, lignin was precipitated in 50 mL 0.01 mol L^{-1} HCl solution and separated by subsequently centrifugation, decantation and drying at 60 °C.

2.4. Esterification of (oxyalkylated) OL

As proof-of-concept, a single-neck round-bottom flask (50 mL) with magnetic stirring bar was filled with ± 0.25 g OL_1 or OL_2 and 5.00 mL propionic acid (≈ 50 equivalents relative to the total OH content) and was placed in a preheated oil bath at 120 °C with a stirring speed of 800 rpm. The reaction took place for 48 h under reflux and afterwards the reaction was quenched by adding tetrahydrofuran and – analogous to the workup procedure of the oxyalkylation – transferred to 200 mL 0.01 mol L^{-1} HCl solution. Immediately after, the solution was filtered with a Buchner filter (Whatman grade 1) and the filter residue was scraped from the filter, placed on a Petri dish and dried in a drying oven (VWR) at 60 °C prior to analysis.

2.5. Characterization techniques

2.5.1. Size exclusion chromatography

An Agilent 1260 Infinity II LC system was used for SEC analysis. The device was equipped with a Polargel-L guard column, two consecutive Polargel-L columns, a UV–VIS and a refractive index detector (RID) in series. The measurements were conducted at 60 °C using DMSO with 0.1 w/v% LiBr as mobile phase at a flow rate of 0.8 mL/min. The calibration was performed with the RI detector using PMMA standards. For the OL feedstock and modified OL, approx. 3.0 – 4.0 mg was dissolved in 1 mL DMSO. All samples were filtered with a syringe filter (0.45 µm) prior to injection and no aggregation was observed for any sample. SEC calibration was done with narrow polymethylmethacrylate standards (PMMA) ranging from 535 g mol^{-1} to 72,000 g mol^{-1} (Agilent Technologies, PSS Polymer Standards Service GmbH).

2.5.2. FTIR spectroscopy

The Fourier-transform infrared spectroscopy (FTIR) spectra of the (modified) lignin samples were obtained with a Shimadzu IRSpirit (equipped with an ATR module made from diamond and a KBr window) with 32 cumulative scans and 2 cm^{-1} resolution within 4000 cm^{-1} – 800 cm^{-1}. All spectra were normalized at ≈1504 cm^{-1} corresponding with C-C stretching vibrations in aromatics [11,23].

2.5.3. Quantitative ^{31}P NMR analysis

^{31}P NMR spectra of lignin samples were recorded with a Bruker 400 MHz Avance II spectrometer equipped with a cryoprobe using inversed gated decoupling (zgig) pulse with 90° pulse angle, 32 scans and a delay time of 10 s combined with ($Cr(acac)_3$) as a relaxation agent, NHND as internal standard and TMDP as phosphorus reagent. The applied ^{31}P NMR protocol was based on the procedure developed by Argyropoulos by dissolving 30.0 mg lignin in 600 µL of a 1/1.6 (v/v) $CDCl_3$/pyridine mixture followed by the addition of 100 µL of a 5 mg mL^{-1} $Cr(acac)_3$ and 18 mg mL^{-1} NHND solution in a 1.5 mL vial with magnetic stirring bar. After overnight stirring, 100 µL TMDP was added and after 2 min homogenization of the sample it was transferred into a 5 mm NMR tube and immediately measured. Postprocessing consisted of manual phase correction and full auto baseline correction [24,25]. The spectra are divided into 4 regions corresponding with the internal standard NHND (151.5 – 152.5 ppm), alOHs (145.0 – 150.0 ppm), phOHs (136.5 – 144.5 ppm) and COOHs (133.5 – 136.0 ppm).

2.5.4. Quantitative ^{13}C NMR analysis

Quantitative ^{13}C NMR spectra of lignin samples were recorded on a Bruker 700 MHz Avance II spectrometer at 40 °C equipped with a cryoprobe using inversed gated decoupling, the zgig90 pulse program, 3072 scans, an acquisition time of 1.4 s and a delay time of 3.0 s [18, 26–28]. The protocol consisted of dissolving ± 100.0 mg lignin sample in 0.5 mL DMSO-d_6 followed by the addition of approximately 10.0 mg 1,3,5-trioxane and adding 60 µL of a ± 50 mg/mL relaxation agent Cr $(acac)_3$. For postprocessing, manual phase correction was performed followed by a full-automatic baseline correction and the DMSO signal was used as a reference at 39.5 ppm.

2.5.5. Attached proton test ^{13}C NMR analysis

Attached Proton Test (APT) ^{13}C-spectra were recorded on a Bruker 700 MHz Avance II spectrometer at 40 °C equipped with a cryoprobe using the J-modulated spin echo (jmod) pulse program, 3072 scans, an acquisition time of 1.4 s and a delay time of 1.0 s. Sample preparation is identical to the quantitative ^{13}C NMR protocol discussed above. The spectra consist of signals in positive phase (CH/CH_3) and opposite (= negative) phase (CH_2 and quaternary C).

2.5.6. ^{1}H-^{13}C HSQC NMR analysis

1H-13C HSQC NMR measurements were performed on a Bruker 400 MHz Avance II spectrometer equipped with a cryoprobe. An hsqcetgpsp.3 pulse program was used with matrices of 2048 data points for the ^{1}H-dimension and 128 data points for the ^{13}C-dimension and resp. spectral widths of 13 to −1 ppm and of 160 to −20 ppm at 298 K. The relaxation delay was set for 1 s with 8 consecutive scans. The lignin samples were solubilized overnight in DMSO-d_6 (100 mg / 600 µL). The solvent signal was used as reference (δ_C 2.50/ δ_H 39.5 ppm) and semi-quantitative analysis was performed by expressing the linkages as a number per 100 aromatic units (= $H_{2,6}/2 + G_2 + S_{2,6}/2$).

3. Results

First, the properties of the different OL feedstocks are discussed (including ^{13}C NMR) followed by the expected OH content after oxyalkylation with resp. $EtCO_3$ and $GlyCO_3$. Next, the modifications with resp. $EtCO_3$ and $GlyCO_3$ are evaluated with ^{31}P NMR and FTIR. The 1,2-diol content after modification with $GlyCO_3$ was determined with both ^{31}P NMR and ^{13}C NMR including a critical discussion with both quantification strategies. Finally, the (oxyalkylated) OL_1 and OL_2 were esterified as a proof-of-concept to illustrate the more accessible alOH groups in comparison with the sterically hindered phOH moieties. For further convenience, lignin products modified with $EtCO_3$ or $GlyCO_3$ are abbreviated as Et-OL_X or Gly-OL_X, respectively and esterified lignins are accompanied with an initial standalone E in the abbreviation (for example E-Et-OL_2 or E-Gly-OL_1).

3.1. Characterization of OL feedstocks

The OL feedstocks were characterized in triplicate (with a 95 % confidence interval (C.I.)) with SEC and ^{31}P NMR. The molecular weight of the highest peak (M_P), number average molecular weight (M_N), weight average molecular weight (M_W) and dispersity (Đ) and numerical values for the concentration of the different OH groups (alOHs, phOHs and COOHs) are shown in Table 1. The molecular weight distributions (MWDs) are visualized in Figure S2 and the FTIR spectra are shown in Figure S3 with the normalized aromatic C=C stretches.

Throughout this study, OL_1 and OL_2 (= beech wood originated lignins) are subjected to a more in-depth analysis using ^{13}C NMR, to gain more insights in the alOH functionalities during oxyalkylation, and an esterification reaction to illustrate the sterically hindered native phOH moieties. Both lignins were available in larger quantities, avoiding the

Table 1
Properties of different OL feedstocks from beech and poplar (95 % C.I.).

Sample	M_P (g mol^{-1})	M_W (g mol^{-1})	Đ	OH functionalities (mmol g^{-1})			
				alOH	phOH	COOH	Total OH
OL_1	6616 ± 28	7836 ± 74	5.0	2.59 ± 0.06	2.43 ± 0.04	0.14 ± 0.02	5.16 ± 0.07
OL_2	3153 ± 73	3664 ± 17	5.1	1.90 ± 0.04	3.04 ± 0.10	0.17 ± 0.02	5.11 ± 0.11
OL_3	6938 ± 276	8372 ± 152	7.5	2.94 ± 0.06	2.28 ± 0.05	0.22 ± 0.02	5.45 ± 0.08
OL_4	6936 ± 160	8441 ± 28	8.4	2.29 ± 0.10	2.52 ± 0.07	0.30 ± 0.01	5.11 ± 0.12

necessity to do multiple in-house laboratory scale organosolv pulping experiments. The ^{13}C NMR spectra of both lignin feedstocks are accessible in Fig. 1 with the integration ranges (indicated in green) to quantify the total alOH content [18]. Oxyalkylation studies identify unreacted native alOH moieties at 58 – 62 ppm after oxyalkylation (with $PrCO_3$ or $GlyCO_3$) [18,26,29]. Yet, for OL feedstocks, extended integration ranges are reported [27,28].

An HSQC of all lignins is available (Figure S4) in order to (1) verify and finetune the integration ranges and (2) identify any overlapping signals which would lead to an overestimation. The integration range 58 – 66 ppm consists of Cγ-OH signals (from *e.g.* β-O-4 and β-5 linkages) and can be used as such [30,31]. Since both lignins primarily consist of β-O-4 linkages (see Table 2), the corresponding Cα-OH signal at 72.3 ppm is important as well but overlaps with the Cγ-O-C signal (71.5 ppm) in the β-β (resinol) linkages [30–33]. However, because of the low resinol (β-β) content in both OL_1 and OL_2, integration over the whole 70.6 – 73.1 ppm range results in an overestimation of alOH contents (especially for OL_1) with resp. 3.22 and 2.36 mmol g^{-1}. By solely integrating the signal at 72.3 ppm (but with interference of other signals), alOH contents of 2.55 and 2.03 mmol g^{-1} are obtained. Deconvolution (see Figure S5) was performed to isolate the Cα-OH contribution (see peak at 72.3 ppm) to improve the quantification, resulting in a lowered native alOH content of 2.45 and 1.97 mmol g^{-1}, resembling with the ^{31}P NMR quantification results (from Table 1).

Table 2
S/G/H units ratio (%) and content of different linkages (per 100 aromatic units) in hardwood lignins.

Sample	S/G/H	β-O-4 (%)	β-β (%)	β-5 (%)
OL_1	65/34/1	27	6	5
OL_2	67/32/1	15	6	4
OL_3	62/36/2	26	5	3
OL_4	59/39/2	22	5	4

While the ^{31}P NMR protocol is a well-established method and measurement time is short (< 10 min with cryoprobe) to quantify OH functionalities in lignin, the preparation of samples for ^{13}C NMR is less complex and less time-consuming while the measurement requires more scans, hence longer measurement time (≈ 4 h with cryoprobe or 20 h with standard probe), due to the low natural abundance of the ^{13}C-

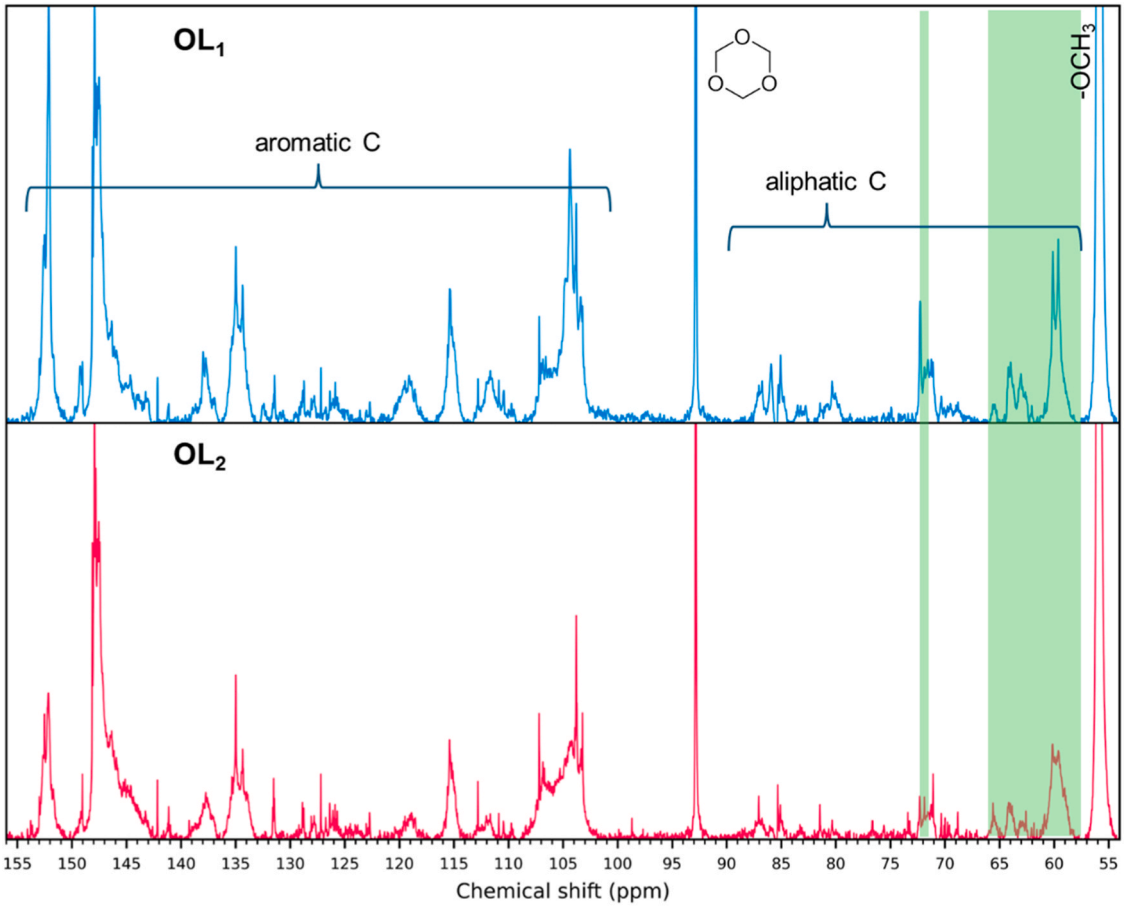

Fig. 1. Quantitative ^{13}C NMR spectra of OL feedstocks (OL_1 and OL_2).

isotope (Table 3). In addition, since lignin is composed of C-atoms, a sufficient high resolution requires a stronger and more expensive high field magnet (700 MHz) in comparison to OH quantification via ^{31}P NMR (400 MHz) and the identification of signals and integration ranges in ^{13}C-spectra is less straightforward. Moreover, with regards to the sample preparation protocol, on one hand the mass of 1,3,5-trioxane as internal standard is rather low thereby increasing the weighing errors while the area of the signal of the internal standard is rather large compared to certain ^{13}C-signals within the lignin structure, hence, the bias between both NMR methods. Several studies report the acetylation of lignin in order to distinguish primary and secondary OH groups in ^{13}C NMR, yet in this work no modification prior to analysis was performed since care must be taken regarding incomplete acetylation and/or fractionation resulting in solubility and loss of material during the work up procedure [27,28,34,35]. These phenomena will affect the obtained OH content besides other structural changes that can occur under such reaction conditions.

3.2. Oxyalkylation of OL feedstocks

Since lignin is a biomacromolecule with thermally unstable linkages (*e.g.* β-O-4) and many attempts to depolymerize lignins into valuable monomers and phOH-rich oligomers are reported, the alkaline environment and thermal treatment applied in the oxyalkylation in here can give rise to the concern of possible depolymerization. However, in our previous publication, we successfully demonstrated the exclusion of unwanted polymerization or condensation reactions at the oxyalkylation conditions [11].

3.2.1. Calculating the theoretical OH content

In previous work, it was established that all OH functionalities in lignin react with $EtCO_3$ – with 0.1 equivalents K_2CO_3 at 150 °C for 30 min – resulting in chain extension by ether and linear carbonate formation [11]. Eq. 1 calculates the relevant expected alOH content whereby the amount of moles of initial OH functionalities does not change but the initial unmodified lignin mass increases (in the denominator) resulting in a lower final alOH content than the unmodified OL feedstocks. The multiplication factors 0.088 g mol^{-1} and 0.044 g mol^{-1} correspond to the M_W of resp. $EtCO_3$ and $EtCO_3$ after decarboxylation with release of CO_2. Remark, if etherification would occur at the alOH moieties, the multiplication factor of 0.088 should be substituted by 0.044 and thereby the theoretical alOH content would further increase. Furthermore, the equation assumes complete conversion of OH functionalities and the absence of side reactions such as repolymerization/condensation or grafting of poly($EtCO_3$) on top of lignin.

$$[\mathrm{alOH}]_{\mathrm{expected}} = \frac{[\mathrm{OH}]_{\mathrm{i,total}}}{1\mathrm{g} + [\mathrm{alOH}]_{\mathrm{i}} * 0.088\frac{\mathrm{g}}{\mathrm{mol}} + \left([\mathrm{phOH}]_{\mathrm{i}} + [\mathrm{COOH}]_{\mathrm{i}}\right) * 0.044\frac{\mathrm{g}}{\mathrm{mmol}}} \quad (1)$$

It was in a previous study elucidated that – in comparison with $EtCO_3$ – only phOH and COOH functionalities react with $GlyCO_3$ – with 0.1 equivalents K_2CO_3 at 175 °C for 30 min – resulting in a lignin with both native alOH functionalities as well as newly formed alOH groups as part of 1,2-diol moieties [11]. Therefore, the numerator in Eq. 2 takes into account that the native alOH groups are not converted in 1,2-diol moieties and subsequently that in the denominator, the mass increase is less substantial than when all OH functionalities are converted. The multiplication factor of 0.074 g mol^{-1} represents the addition of $GlyCO_3$ after decarboxylation with release of CO_2. Remark that Eqs. 1 and 2 both calculate the final alOH content which is equal to the total OH content since no phOH and COOH moieties are left over after reaction.

$$[\mathrm{alOH}]_{\mathrm{expected}} = \frac{\left([\mathrm{phOH}]_{\mathrm{i}} + [\mathrm{COOH}]_{\mathrm{i}}\right) * 2 + [\mathrm{alOH}]_{\mathrm{i}}}{1\mathrm{g} + \left([\mathrm{phOH}]_{\mathrm{i}} + [\mathrm{COOH}]_{\mathrm{i}}\right) * 0.074\frac{\mathrm{g}}{\mathrm{mmol}}} \quad (2)$$

For both modifications with $EtCO_3$ and $GlyCO_3$, the final OH content consists of solely alOH functionalities whereby the modified lignin with $GlyCO_3$ will consist of native alOH functionalities and 1,2-diols. The expected total OH contents (= expected final alOH contents) are listed in Table 4 and are subsequently used to evaluate the experimental results which are discussed in the following sections.

3.2.2. Modification with ethylene carbonate

In comparison with the modification with $GlyCO_3$, the reaction with $EtCO_3$ did not result in a noticeable viscosity increase during the work up procedure (specifically during the transfer of the content from the round-bottom flask to the 0.01 mol L^{-1} HCl solution) since the reactant cannot react with itself (in comparison to $GlyCO_3$ with poly($GlyCO_3$) formation) [11]. The results of the oxyalkylation of the different OL_X with $EtCO_3$ are visualized in Fig. 2 with complete conversion of native phOH and COOH moieties at 150 °C (by release of CO_2 proven by correlating CO_2 production and decrease in OH content by Liu *et al.*) [36]. In the FTIR spectra (Figure S6), a signal arises after ethoxylation at ≈ 1740 cm^{-1} corresponding to linear carbonates. These linear carbonates are formed in the reaction between native (or newly formed) alOH groups and $EtCO_3$ [12,37–39]. Thus, all different OH functionalities of lignin take part in the oxyalkylation with $EtCO_3$ and moreover complete conversion was observed since the final alOH contents after oxyalkylation are similar to the expected OH contents in Table 4 (and visualized in Fig. 2). The proposed assumptions are, therefore, justifiable and applicable in the experimental approach with (almost) complete conversion of all OH functionalities and no (or barely any) occurrence of side reactions. Thus, the measured total alOH content with ^{31}P NMR fully consists of newly created primary alcohols. The FTIR spectra, moreover, show increased signal intensity at 2750 – 3000 cm^{-1} corresponding with sp^3-hybridized C-H stretching indicating successful oxyalkylation. Quantitative ^{13}C NMR (Figure S7) was performed on Et-OL_1 and Et-OL_2 to verify the ^{31}P NMR results by integrating the 58 – 62 ppm region of newly formed primary C-OH signals (based on a study by Duval *et al.* via HSQC NMR) [12] and integration of the signal of the remaining Cα-OH in β-O-4 bonds. The total aliphatic OH content amounts 3.93 and 3.77 mmol g^{-1}, respectively. These values are slightly higher than the ^{31}P NMR data because of overlap in the Cα-OH region (≈ 72.3 ppm) as can be seen in the HSQC NMR spectra in Figure S8. Moreover, the ^{13}C NMR spectra show only a very small signal present, thus the majority of native Cα-OHs were converted.

However, it is necessary to remain critical about the obtained results. For example, Duval *et al.* ethoxylated Kraft lignin at low reaction temperatures of 100 °C – 110 °C for 3 h. Their data supports (**1**) only partial conversion of primary and secondary alOHs in lignin; (**2**) primarily etherification instead of esterification and (**3**) chain extension by grafting of hydroxyethyl side chains (via linear carbonates) [12]. Our HSQC NMR spectra of Et-OL_1 and Et-OL_3, in Figure S8, show an upfield shift of the β-signal in β-O-4 linkages due to modification/ethoxylation of α- and/or γ-OHs. Yet, a signal is still visible (δ_H 4.9: ppm /δ_C 72.3 ppm) which corresponds to the remaining α-OHs. Therefore, the small bias between the experimental and theoretical OH content in this

Table 3
Strengths and weaknesses of both quantitative ^{31}P NMR and ^{13}C NMR of lignins.

	^{31}P NMR	^{13}C NMR
Sample preparation	Difficult	Easy
Measurement time	Short (< 30 min)	Long (4 h – 20 h)
Resolution	Medium field (400 MHz)	High field (700 MHz)
Spectra and integration	Well-known	Less straightforward

Table 4
Expected OH content after modification with $EtCO_3$ and $GlyCO_3$.

OL feedstock	OL_1	OL_2	OL_3	OL_4
$[OH]_{expected}$ with $EtCO_3$ (Eq. 1)	3.85	3.90	3.98	3.85
$[OH]_{expected}$ with $GlyCO_3$ (Eq. 2)	6.49	6.72	6.70	6.56

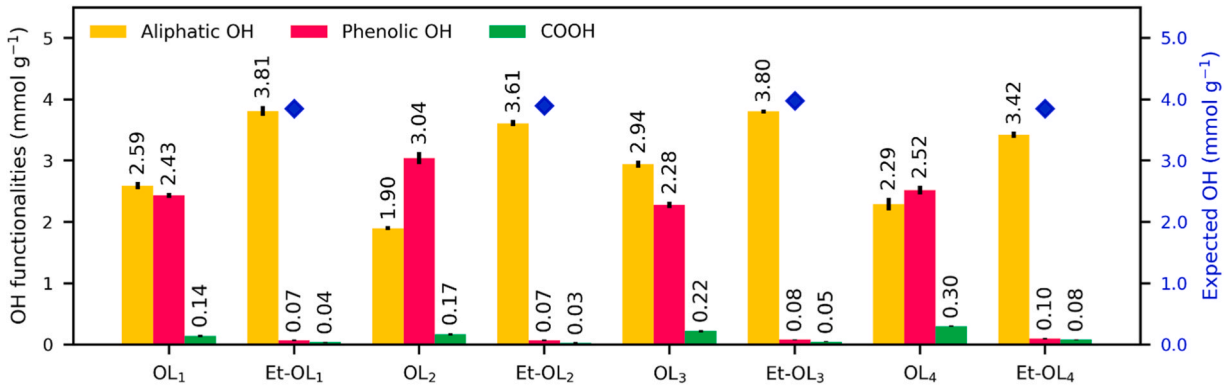

Fig. 2. Content of different OH moieties (determined with ^{31}P NMR) and the expected OH content after oxyalkylation with $EtCO_3$ at 150 °C.

study (Fig. 2) can be caused by the non-conversion of native alOHs while the phOHs are converted and grafting of hydroxyethyl side chains further lowers the final alOH content, reaching the theoretical values. However, certain remarks with this hypothesis are important to make: (**1**) Duval *et al.* performed the modification at a much lower reaction temperature, thereby affecting the conversion degree, reactivity of certain OH groups and reaction pathway and side reactions (*e.g.* decarboxylation) [11,26]; (**2**) the HSQC NMR spectra show great complexity and overlap of signals; (**3**) quantification utilizes H/G/S-unit signals as internal standard, yet the ratio changes after oxyalkylation for both $EtCO_3$ (with the largest change in ratio) and $GlyCO_3$ and finally (**4**) our quantitative ^{13}C NMR results show the majority of α-OHs are converted. Therefore, we can conclude that the ethoxylation in this study (almost) completely converted all OH functionalities with no (or barely any) occurrence of side reactions.

Important to remark is the small difference, see Fig. 2, that exists between the experimental and theoretical alOH content for Et-OL_2, Et-OL_3 and Et-OL_4 with slightly lower experimental alOH contents than the theoretically calculated (and expected) alOH contents. Especially with OL_2 and OL_4, a higher bias is present which cannot be related to the concerned feedstock properties. For example, phOH and COOH functionalities react more easily (because of the lower pK_a value) than alOH moieties, yet OL_2 and OL_4 have higher phOH and lower alOH contents than OL_1 and OL_3. Therefore, the bias is likely to be caused by limited grafting of poly($EtCO_3$) on top of lignin OH functionalities or condensation/repolymerization, though the latter was considered in previous work to optimize the reaction conditions but was not detected [11]. Moreover, condensation/repolymerization would severely increase the molar mass, yet both the increase in M_P and M_W is larger for Et-OL_1 than for Et-OL_3 and Et-OL_4 (see Table S1). Thus, the lower alOH content is not caused by condensation/repolymerization. It is important to note that SEC is a less reliable technique for the analysis of oxyalkylated lignins. Lignin has an aromatic backbone and oxyalkylation with $EtCO_3$ leads to long aliphatic chains (especially if grafting of poly($EtCO_3$) occurs), hence changing its chemical structure and its hydrodynamic behavior. Therefore, comparing lignins before and after modification is less valid. Furthermore, these long aliphatic chains can go partially inside the pores of the stationary phase, thereby increasing the retention time. This would lead to underestimated molecular weight values. In addition, the M_W values suffer from a fraction not within the calibration range and column specifications and the M_P is not a calculated average. The hypothesis that the ethoxylation for the latter three feedstocks has progressed slightly too far (newly formed alOH groups limitedly react), is in correspondence with (**1**) the already determined modification of alOH moieties (FTIR signal at 1740 cm^{-1}) and (**2**) the high reactivity attributed to $EtCO_3$ [26]. In future experiments, a slight reduction in reaction time would likely avoid the slightly lower OH content than theoretically expected.

Interestingly, both OL_2 and OL_4 have the same initial total OH content before modification. Since it is assumed that all OH functionalities take part in the reaction, the same final alOH content after reaction must be achieved. Yet, care must be taken that phOH and alOH moieties react differently with a higher increase in molar mass when alOH moieties react, and therefore, Et-OL_2 and Et-OL_4 have a different final alOH content (of resp. 3.61 and 3.42 mmol g^{-1}). In order to determine the content of newly formed alOH functionalities, ^{31}P NMR is sufficient as a fast quantification method (after phosphorylation) since all native OH moieties were converted.

3.2.3. *Modification with glycerol carbonate*

The results of the oxyalkylation at 175 °C of the different OLs with $GlyCO_3$ are visualized in Fig. 3. A complete conversion of the phOH and COOH moieties was achieved while the native alOH content could not be quantified. Yet, previous research has proven that alOHs likely do not react with $GlyCO_3$ for example because the absence of a linear carbonate signal in FTIR (≈ 1740 cm^{-1}) which is reported in other studies and was noticed in this work as well for all lignins (Figure S9) [11,23]. The expected/predicted OH content was not achieved (based on Eq. 2) which is different than with the modification with $EtCO_3$. The lower obtained alOH contents in here are not caused by the non-reactivity of native alOH moieties with $GlyCO_3$ since this was taken into account in Eq. 2. The bias is partially due to the occurrence of a side-reaction, namely the grafting of cyclic carbonates on top of lignin as this phenomenon was determined in previous work and by other studies whereby it was shown that a minority of the 1,2-diols are converted by the internal transesterification [11,23,37,40].

This side reaction was further proven by the presence of a signal at ≈ 1790 cm^{-1} in all Gly-OL_X samples. Moreover, the intensity of this signal relative to the aromatic C=C stretching vibrations (1.254 and 1.548 for resp. Gly-OL_1 and Gly-OL_2) reveals a high content of cyclic CO_3 for Gly-OL_2 and is an important observation with regards to the low alOH content specifically in Gly-OL_2. Indeed, besides the general low alOH content for all modified lignin feedstocks, the theoretically calculated alOH content with Eq. 2 for Gly-OL_2 should be higher than for Gly-OL_1, however this trend is not present. Since OL_2 contains the most initial phOH functionalities, a higher 1,2-diol content should be obtained resulting in a statistically higher possibility to form cyclic carbonate functionalities. To further verify, $GlyCO_3$-modified lignin was further hydrolyzed to quantify the cyclic CO_3 content with ^{31}P NMR revealing (and supporting FTIR measurements) a high cyclic CO_3 content in Gly-OL_2 (0.64 mmol g^{-1}) and lower content in Gly-OL_1 (0.42 mmol g^{-1}). In addition, a possible explanation is that part of the OL_2 feedstock (whether or not modified) was lost during the work up procedure because of the low M_W (≈ 3700 g mol^{-1}) with likely a higher monomer, dimer and trimer content than compared to the M_W of the other lignins (≈ 8000 g mol^{-1}) which can cause lower obtained alOH contents. This hypothesis is further discussed in Section 3.2.3.1. For all oxyalkylated lignin products, sharp signals at ≈ 1120 cm^{-1}, 1050 cm^{-1}

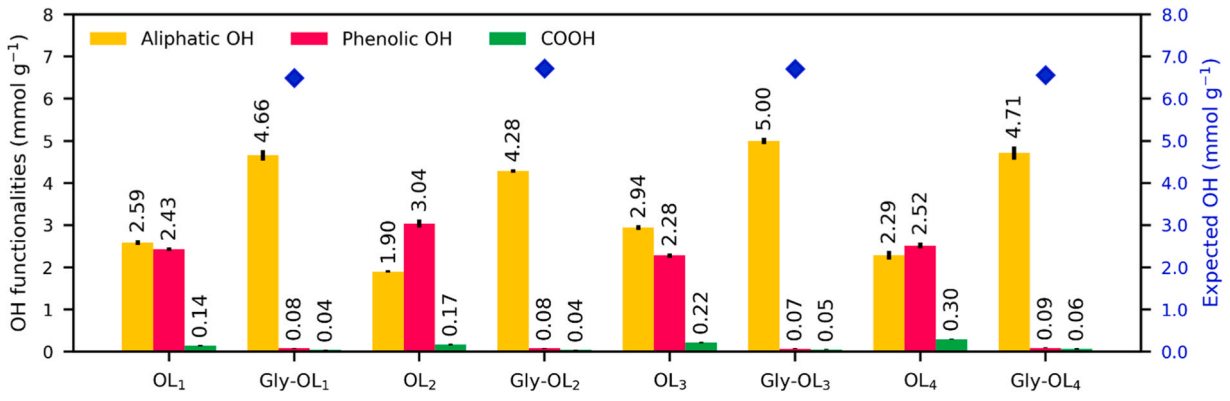

Fig. 3. Content of different OH moieties (determined with ^{31}P NMR) and the expected OH content after oxyalkylation with $GlyCO_3$ at 175 °C.

and ≈ 1030 cm^{-1} arise corresponding with secondary alcohols, C-O alkyl ethers in alkyl aryl ethers and primary alcohols in the FTIR spectra in Figure S9 [11]. In addition, the HSQC NMR spectra of Gly-OL$_1$ and Gly-OL$_3$ (Figure S10) reveal a similarity with the HSQC NMR spectra obtained after ethoxylation (Figure S8) besides increasing complexity: an upfield shift of the β-signal in β-O-4 linkages due to modification/oxyalkylation of α- and/or γ-OHs. Yet, a signal is still visible (at δ_H 4.9: ppm /δ_C 72.3 ppm) which corresponds to the remaining α-OHs. Furthermore, the ^{13}C-^{1}H signals of the 1,2-diol functionalities are indicated in Figure S10 and will be discussed more in depth in Section 3.2.3.3.

3.2.3.1. Investigating loss of low molecular weight fragments. While loss of low molecular weight fragments was not perceived in the modification with $EtCO_3$ with experimental values resembling theoretical expectations, modification with $GlyCO_3$ results in a more polar and soluble polyol in polar solvents such as water with increasing alOH groups. Moreover, the work up procedure explicitly keeps the precipitated lignin in solution for half an hour to avoid trapped $GlyCO_3$. In Figure S11, Gly-OL$_1$ (blue) has clearly shifted to higher molecular weights compared with OL$_1$, yet the shape rather remains identical. With Gly-OL$_2$ (red), a similar shift is present to higher molecular weights, yet the shape is less similar to the OL$_2$ feedstock. In order to verify whether loss of monomers/dimers/… in the work up procedure partially causes the bias between theoretical and experimental alOH contents after oxyalkylation, low molecular weight fragments were removed prior to oxyalkylation to remove the possible root cause. Both OL$_1$ and OL$_2$ were fractionated in order to solely obtain precipitable molecules by dissolving feedstock into a 0.01 mol L^{-1} HCl solution to mimic the work up procedure of the oxyalkylation. The fractionated OL$_1$ and OL$_2$ had an M_W of approx. 8000 and 3700 g mol^{-1}, respectively, indicating barely any loss of unmodified lignin with very similar OH moieties (see Table S2) and the MWDs are very alike the feedstocks (Figure S11).

An additional fractionation was performed with ethyl acetate and solely macromolecular OL$_1$ and OL$_2$ feedstocks (see MWDs in Figure S11) were obtained with high molecular weights (Table S2). Interesting is the decrease in phOH content for both ethyl acetate fractionated OL$_1$ and OL$_2$ indicating predominant solubility of phOH containing molecules. Because of the altered OH content, the theoretical expected values were recalculated by Eq. 2 with resp. 5.95 and 6.66 mmol g^{-1}. After successful oxyalkylation with a clear shift to high molecular weights in the MWDs in Figure S11, the alOH contents are 4.37 and 4.19 mmol g^{-1}, thus obtaining lower alOH contents than without fractionation but still not meeting the theoretically expected alOH contents. Thereby, the hypothesis that the bias between theoretical and experimental alOH contents is caused by loss of low molecular weight fragments, is rejected since a substantial bias is still present even with the fractionated lignin feedstocks. However, fractionation prior to oxyalkylation can still be interesting. For example Sternberg *et al.* fractionated lignin oil with heptane to isolate dimers and oligomers of higher functionality to avoid chain-termination in non-isocyanate polyurethane synthesis [41].

3.2.3.2. Determining the 1,2-diol content with ^{31}P NMR. While the alOH content was determined above after modification with $EtCO_3$ and $GlyCO_3$ (since all products exclusively contain alOHs), the alOH functionalities obtained by ethoxylation are all primary (aliphatic) alcohols [39] which is different after $GlyCO_3$ modification with a mixture of primary alcohols (native alOHs and alOHs part of the 1,2-diol) and secondary alcohols (part of the 1,2-diol). The following sections discuss the 1,2-diol content determination by using ^{31}P NMR and ^{13}C NMR spectroscopic techniques. As a benchmark, the theoretical 1,2-diol content was calculated (Eq. 3) assuming no conversion of native alOH functionalities and no occurrence of side reactions. The multiplication factor of 0.074 g mol^{-1} in Eq. 3 represents the addition of $GlyCO_3$ after decarboxylation with release of CO_2.

$$[1,2-\mathrm{diol}]_{\mathrm{expected}} = \frac{[\mathrm{phOH}]_i + [\mathrm{COOH}]_i}{1\mathrm{g} + \left([\mathrm{phOH}]_i + [\mathrm{COOH}]_i\right) * 0.074 \frac{\mathrm{g}}{\mathrm{mmol}}} \quad (3)$$

With experimental ^{31}P NMR, there is overlap between native and newly formed alOHs in the spectra, therefore it is not straight-forward to determine the vicinal diol content. An equation was elucidated which solely uses ^{31}P NMR data to (indirectly) determine the 1,2-diol content. First, it is important to establish the fact that the molar mass of lignin increases with the oxyalkylation: $GlyCO_3$ alters the structure of lignin with conversion of OH functionalities in – specifically – alOH moieties which are part of a 1,2-diol conformation and thereby the molar mass of lignin changes. The resulting mass increase – upon the initial mass of 1 g – can be determined by using the following equations with Eq. 4 assuming complete OH conversion (with final mass = 1.4974 g) and whereby Eq. 5 only assumes phOH and COOH conversion (with final mass = 1.1894 g).

$$m_{f-\mathrm{oxy(full)}}\ (\mathrm{g}) = 1\mathrm{g} + [\mathrm{alOH}]_i\ * 0.118 \frac{\mathrm{g}}{\mathrm{mmol}} + \left([\mathrm{phOH}]_i + [\mathrm{COOH}]_i\right) * 0.074 \frac{\mathrm{g}}{\mathrm{mmol}} \quad (4)$$

$$m_{f-\mathrm{oxy(partial)}}\ (\mathrm{g}) = 1\mathrm{g} + \left([\mathrm{phOH}]_i + [\mathrm{COOH}]_i\right) * 0.074 \frac{\mathrm{g}}{\mathrm{mmol}} \quad (5)$$

It is important to emphasize that the above equations make three important assumptions: **(1)** any reactive OH functionality is completely converted while unreactive OH functionalities do not react at all; **(2)** decarboxylation goes along with release of CO_2 and **(3)** no side reactions take place which substantially alter the initial mass of lignin feedstock (*e.g.* grafting of poly($GlyCO_3$)). Next, it is possible to calculate the 1,2-diol content if complete conversion of all OH functionalities takes

place by simply dividing the final alOH content by a factor of 2 (Eq. 6). In this case, only alOH moieties are present within the modified lignin structure which are part of a 1,2-diol.

$$[1,2-\text{diol}] = \frac{[\text{alOH}]_f}{2} \quad (6)$$

However, when not all OH functionalities are converted into alOH functionalities, it is more difficult to grasp the final 1,2-diol content. For example, in the case of this study, native alOH groups (not part of a 1,2-diol conformation) do not (or only limitedly react) with $GlyCO_3$, therefore Eq. 6 can be altered (Eq. 7) whereby the numerator considers the initial alOH content.

$$[1,2-\text{diol}] = \frac{\Delta[\text{alOH}]_{f-i}}{2} = \frac{[\text{alOH}]_f - [\text{alOH}]_i}{2} \quad (7)$$

However, Eq. 7 is not completely accurate since it assumes that the initial alOH content does not change after oxyalkylation, yet since the molar mass increases, the initial alOH content will have decreased (similar to a dilution factor) and should be taken into account. Therefore, the dilution of the initial alOH content ($[\text{alOH}]_i$) is taken into account by Eq. 8 and abbreviated with $[\text{alOH}]_{i(f)}$ which stands for the initial alOH content corrected with the mass increase ($= m_{f-oxy(partial)}$) after oxyalkylation if only phOH and COOH groups are converted. After taking into account the mass increase (according to Eq. 5), the initial alOH content in the final product is 2.19 mmol g^{-1}.

$$[\text{alOH}]_{i(f)} = \frac{[\text{alOH}]_i * 1g}{m_{f-oxy(partial)}} \quad (8)$$

To finally calculate the 1,2-diol content, Eq. 8 is substituted in Eq. 7 resulting in Eq. 9 with a 1,2-diol content for Gly-OL_1, Gly-OL_2, Gly-OL_3 and Gly-OL_4 of resp. 1.24; 1.37; 1.26 and 1.41 mmol g^{-1}. These values are obtained from indirect ^{31}P NMR data because several calculations were made to enhance the accuracy of the 1,2-diol content, thereby making an attempt to correct for overlapping signals in the spectra. It is important to emphasize several assumptions were made that overall will likely result in an underestimation since $m_{f\text{-}oxy\ (2)}$ is an ideal but minimal mass increase: any occurring side reaction (cyclic CO_3 groups or condensation/repolymerization) will result in a higher mass increase and subsequently a higher 1,2-diol content.

$$[1,2-\text{diol}] = \frac{[\text{alOH}]_f - [\text{alOH}]_{i(f)}}{2} = \frac{[\text{alOH}]_f - \frac{[\text{alOH}]_i * 1g}{m_{f-oxy(partial)}}}{2} \quad (9)$$

In addition, the 1,2-diol content of 1.37 mmol g^{-1} for Gly-OL_2 is likely an overestimation since the ^{31}P NMR data specifically revealed a substantially lower alOH content (compared to the other modified lignins). The reason for the lower OH content is not yet attributed to a root cause but is not caused by loss of low molecular weight fragments as this was investigated in Section 3.2.3.1. Thereby, the content determined via ^{31}P NMR is less reliable as certain assumptions can be falsely accepted in this case, leading to a wrong 1,2-diol content.

3.2.3.3. Quantitative ^{13}C NMR. To quantify the 1,2-diol content via a direct measurement, ^{13}C NMR was chosen as several publications report clear and distinguished signals representing carbons bonded to newly formed hydroxyl groups after oxyalkylation with cyclic carbonates [26,29,42]. Most available literature focusses on the reaction with other cyclic carbonates such as $EtCO_3$ and $PrCO_3$, resulting in a gap in knowledge when it comes to the interpretation of signals in ^{13}C-spectra. A successful oxyalkylation with $GlyCO_3$ results in a vicinal diol which consists of a methylene and methine carbon bonded to one of the (new) OH groups. An APT ^{13}C-analysis was performed on Gly-OL_1 (Figure S12) to provide multiplicity insights of the C-signals thereby allowing the possibility to distinguish signals corresponding with either quaternary and methylene carbon (-CH_2-) signals or methine (-CH<) and methyl carbon (-CH_3) signals. Additionally, PerkinElmer ChemDraw Professional (v22.2.0.3300) software was used to estimate the shifts of the signals on the x-axis (Figure S13). The 1,3-diol functionalities were taken into consideration as well, yet no signals were visible at 41.6/41.7 ppm (Figure S14). However, it is possible that the signal overlaps with the broad DMSO-d_6 signal, especially if the signal-to-noise ratio is low (*i.e.* a low 1,3-diol content). Therefore, HSQC NMR spectra of Gly-OL_1 and Gly-OL_3 were evaluated since the signal of the methine (CH) in the 1,3-diol would be well separated from the DMSO-d_6 signal in the ^1H-axis (1.5 – 2.0 ppm). No signal (see red square in Figure S10) was visible indicating the absence of 1,3-diols and can be explained by the sterically hindered methine carbon (CH) of $GlyCO_3$ in the oxyalkylation.

By combining above information, the total alOH content was determined by integrating the native alOH functionalities region including the methylene carbon of the 1,2-diol (57.5 – 64.6 ppm) + the signal at (70.3 – 71.0 ppm) corresponding with the methine carbon of the 1,2-diol + the signal of the Cα-OH signal at 72.3 ppm. This results for Gly-OL_1 and Gly-OL_2 to a total alOH content of resp. 4.69 and 4.19 mmol g^{-1} which are in good agreement with ^{31}P NMR (4.66 and 4.28 mmol g^{-1} respectively). However, it is important to emphasize the complexity with the ^{13}C NMR spectra, for example a new signal arises at 64.5 – 66.4 ppm which interferes with the native alOH region and therefore the integration range was limited to 57.5 – 64.6 ppm (see HSQC NMR spectrum in Figure S15, whereby two distinct signals – split in the ^1H-axis – are visible at 64.5 – 67.0 ppm on the ^{13}C-axis).

The 1,2-diol content was determined by integrating the methylene carbon (of the 1,2-diol) signal at 62.3 – 63.5 ppm and the methine carbon (of the 1,2-diol) signal at 70.3 – 71.0 ppm, resulting in a 1,2-diol content of resp. 1.49 and 1.27 mmol g^{-1}. However, the signal of the methine carbon suffers from other signals resulting in a too high content. After deconvolution (Figure S16), the 1,2-diol content is respectively 0.98 and 0.76 mmol g^{-1}. Remarkably, the 1,2-diol content determined via both NMR methods (Table 5) is – especially for OL_2 – substantially different and is likely caused by falsely accepted assumptions within the ^{31}P NMR method, thus, ^{13}C NMR is likely more reliable. Moreover, the content of grafted cyclic carbonate groups formed by internal transesterification can be quantified at 155.5 ppm to be 0.47 mmol g^{-1} for Gly-OL_1 and 0.74 mmol g^{-1} for Gly-OL_2 [41]. Both cyclic carbonate content values resemble the numerical values obtained after hydrolysis of the ring structure and subsequent ^{31}P NMR analysis (Table 5), discussed in Section 3.2.3. As a verification, the signal at 155.5 ppm (in APT – Figure S12) was negative therefore indicating either a methylene or quaternary carbon. However, in Figure S17, in the y-axis ($= ^{13}C$) from the HSQC measurement (projected on the x-axis to obtain a ^1D spectrum for convenience), the signal was absent. As a consequence, this signal specifically corresponds to a quaternary carbon which further proofs that it belongs to the carbonyl carbon of the cyclic CO_3 functionality [18].

3.3. Esterification of OL and modified OL

As a proof-of-concept, the OL_1 and OL_2 feedstocks and subsequently oxyalkylated products (Et-OL_1, Et-OL_2, Gly-OL_1 and Gly-OL_2) were evaluated in the sustainable and direct esterification with propionic acid to illustrate the improved uniform functionality and reactivity and more accessible newly formed alOH groups than the native OH functionalities, important for thermoset development [7,9,10,12,19,20,39]. Moreover, oxyalkylation enhances the thermal stability of lignin with higher $T_{d5\ \%}$

Table 5
Comparison of results from quantitative ^{13}C NMR and ^{31}P NMR.

	1,2-diol content (mmol g^{-1})		Cyclic carbonates (mmol g^{-1})	
Sample	**Gly-OL_1**	**Gly-OL_2**	**Gly-OL_1**	**Gly-OL_2**
^{31}P NMR	1.24	1.37	0.42	0.64
^{13}C NMR	0.98	0.76	0.47	0.74

(temperature at which 5 % of the sample's weight is lost due to thermal decomposition determined by thermogravimetric analysis), thereby improving the processability of lignin in thermoplastics [20,28]. Esterified lignins can be beneficial in lignin characterization as solubility of lignin is often a hurdle in appropriate solvents for analysis (tetrahydrofuran (THF) as a SEC solvent or $CDCl_3$ in ^{31}P NMR) [28,43–46]. By reducing the hydrogen bonding and introducing hydrophobic alkyl chains by esterification (or acetylation), solubility in apolar solvents like THF increases. Besides solubility, miscibility and compatibility can also result in a setback in lignin applications with inhomogeneous lignin/polymer blends which can be improved by esterification [2,21,47]. Moreover, unmodified lignin can be used as a cheap filler material, thereby not fully benefiting from lignins' properties and possibilities but increasing the bio-based content of the material. Esterified lignins, on the other hand, can be used as filler material with additional plasticizing effect and potentially improving certain product properties and specifications, thereby allowing a higher substitution degree of fossil-based chemicals with bio-based lignins.

In a first step, the temperature of the esterification was evaluated by using a temperature of 100 °C and 120 °C for 48 h to esterify OH functionalities in OL_1 and OL_2 (see Fig. 4). A sufficiently high temperature is necessary to evaporate water during the reaction and to lower the pK_a of propionic acid [47]. At 100 °C, a substantial decrease of ≈ 72 % in alOH content for both OL feedstocks was observed accompanied with a minor phOH decrease of 25 % for OL_1 and 15 % for OL_2. An increase in temperature up to 120 °C, gave a roughly similar decrease in phOH content (24 %), while the alOH content substantially decreased by ≈ 90 %. Therefore, a temperature of 120 °C is optimal for esterification of alOH functionalities. The FTIR spectra (Figure S18) support NMR measurements with a decrease in O-H signal intensity, yet still present because of the residual phOH moieties. The signal at ≈ 1735 cm^{-1} corresponds with the C═O stretch in esters and is clearly more intense at the highest temperature for both lignins.

Next, the optimal temperature of 120 °C was applied to modify the oxyalkylated products with $EtCO_3$ and $GlyCO_3$ with almost complete conversion of alOH functionalities (Fig. 5), thereby clearly illustrating the importance of converting sterically hindered phOH moieties into easily accessible alOH functionalities. Moreover, in the FTIR spectra in Figure S19, the absence of the O-H stretch signals illustrates the high esterification degree together with an intense signal of the carbonyl bond in esters (in comparison with the esterified OL feedstocks).

4. Conclusion

In this research, two beech OL and two poplar OL feedstocks were successfully modified with both $EtCO_3$ and $GlyCO_3$ based on the protocol of a previous study at resp. 150 °C and 175 °C with K_2CO_3 as catalyst. The modification with $EtCO_3$ resulted in a complete conversion of native OH functionalities leading to a lignin solely consisting of primary alOH functionalities. However, three out of four modified lignins showed a slightly lower OH content which is attributed to limited grafting of poly($EtCO_3$) on top of lignin OH functionalities, thus the reaction progressed slightly too far. The modification with $GlyCO_3$ only converted the phOH and COOH groups. An internal transesterification as side reaction occurred leading to final cyclic CO_3 moieties on top of lignin. These cyclic CO_3 groups were quantified by conducting hydrolysis and subsequent ^{31}P NMR (for Gly-OL_1 and Gly-OL_2 resp. 0.42 and 0.64 mmol g^{-1}) and these results were supported by quantitative ^{13}C NMR (for Gly-OL_1 and GlyOL_2 resp. 0.47 and 0.74 mmol g^{-1}). In addition, both ^{13}C NMR and ^{31}P NMR were used to either directly or indirectly quantify the 1,2-diol content and to evaluate the experimentally obtained values with theoretically calculated ones. Since ^{31}P NMR relies on several assumptions and calculations as an indirect measurement, ^{13}C NMR is the preferable technique yet suffers from a complex and not yet fully understood spectrum as well as the necessity to deconvolute in order to isolate overlapping signals. Finally, as a proof-of-concept, the modified lignins were esterified with propionic acid at an optimized temperature of 120 °C for 48 h. The almost complete conversion of new and original alOH moieties clearly demonstrates that oxyalkylation is a very viable method to obtain a more uniform and reactive lignin with easily accessible OH groups for the green esterification, and more general, for thermoset development such as polyurethanes.

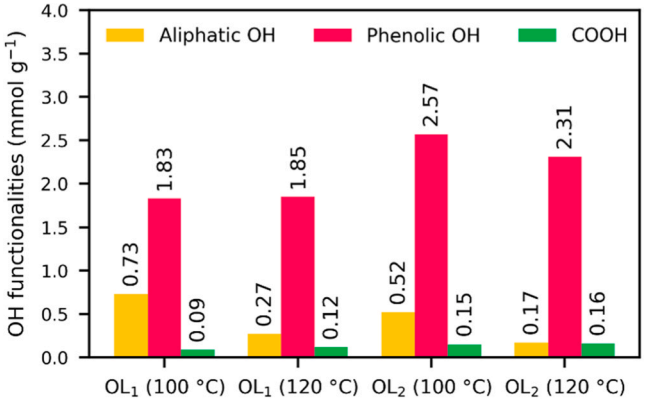

Fig. 4. Content of different OH moieties (determined with ^{31}P NMR) after esterification of OL_1 and OL_2 feedstocks at 100 °C or 120 °C with propionic acid.

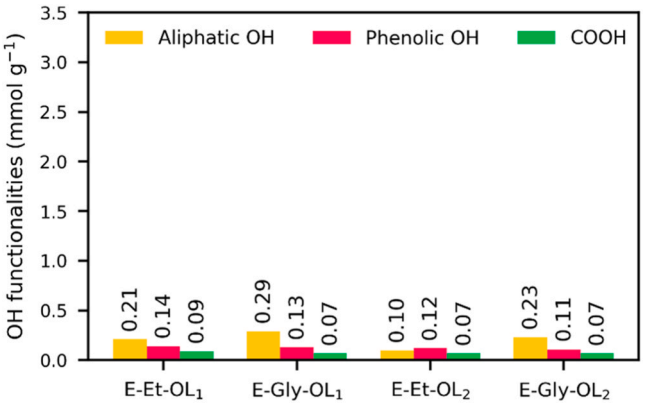

Fig. 5. Content of different OH moieties (determined with ^{31}P NMR) after esterification of modified lignins at 120 °C with propionic acid.

Statements & declarations

B.J. acknowledges the Research Foundation Flanders (FWO) for financial support through grant 1S75824N. We thank the NMR Expertise Centre (Ghent University) for providing support and access to its NMR infrastructure and researcher Boyana Atanasova from the INCAT group to provide in-house extracted lignin from poplar.

Declaration of Competing Interest

The authors declare that they have no known competing financial interests or personal relationships that could have appeared to influence the work reported in this paper.

Appendix A. Supporting information

Supplementary data associated with this article can be found in the online version at doi:10.1016/j.nxmate.2025.101279.

Data availability

Data will be made available on request.

References

[1] A. Slabon, B.V.M. Rodrigues, To break, or not to break: is selective depolymerization of lignin a riemann hypothesis rather than a solution? Green. Chem. 27 (8) (2025) 2178–2183, https://doi.org/10.1039/D4GC05439C.

[2] B. Jacobs, et al., Sustainable lignin modifications and processing methods - Green chemistry as the way forward, Green. Chem. 25 (2023) 2042–2086, https://doi.org/10.1039/D2GC04699G.

[3] Q. Hua, et al., Functional lignin building blocks: reactive vinyl esters with acrylic acid, Biomacromolecules 24 (2) (Feb. 2023) 592–603, https://doi.org/10.1021/acs.biomac.2c00806.

[4] S. Laurichesse, L. Avérous, Chemical modification of lignins: towards biobased polymers, Prog. Polym. Sci. 39 (7) (Jul. 2014) 1266–1290, https://doi.org/10.1016/J.PROGPOLYMSCI.2013.11.004.

[5] Y. Lee, P. Chang-Ho, E. Y, Lee, Chemical modification of Methanol-Insoluble kraft lignin using oxypropylation under mild conditions for the preparation of bio-polyester, J. Wood Chem. Technol. 37 (5) (Sep. 2017) 334–342, https://doi.org/10.1080/02773813.2017.1303512.

[6] X. Zhang, et al., Rigid polyurethane foams containing lignin oxyalkylated with ethylene carbonate and polyethylene glycol, Ind. Crops Prod. 141 (2019) 111797, https://doi.org/10.1016/j.indcrop.2019.111797.

[7] J. Sternberg, O. Sequerth, S. Pilla, Green chemistry design in polymers derived from lignin: review and perspective, Prog. Polym. Sci. 113 (Feb. 2021) 101344, https://doi.org/10.1016/j.progpolymsci.2020.101344.

[8] D. Winfield, J. Ring, J. Horn, E.M. White, J. Locklin, Semi-aromatic biobased polyesters derived from lignin and cyclic carbonates, Green. Chem. 23 (23) (2021) 9658–9668, https://doi.org/10.1039/D1GC03135J.

[9] A. Eraghi Kazzaz, Z. Hosseinpour Feizi, P. Fatehi, Grafting strategies for hydroxy groups of lignin for producing materials, Green. Chem. 21 (21) (2019) 5714–5752, https://doi.org/10.1039/C9GC02598G.

[10] K. Dunne, E.K. Acquah, T. Allohverdi, R. Schenck, M. Nejad, Technical lignin-derived liquid polyols for flexible polyurethane foam in automotive seating (no. n/a), Biofuels Bioprod. Bioref. 19 (Mar. 2025) 894–910, https://doi.org/10.1002/bbb.2750.

[11] B. Jacobs, et al., Bio-polyol chemical design for self-healing boronate ester gels by Green oxyalkylation of organosolv lignin, Eur. Polym. J. 228 (2025) 113846, https://doi.org/10.1016/j.eurpolymj.2025.113846.

[12] A. Duval, W. Benali, L. Avérous, Turning lignin into a recyclable bioresource: transesterification vitrimers from lignins modified with ethylene carbonate, Green. Chem. 26 (14) (2024) 8414–8427, https://doi.org/10.1039/D4GC00567H.

[13] A. Salanti, L. Zoia, M. Orlandi, Chemical modifications of lignin for the preparation of macromers containing cyclic carbonates, Green. Chem. 18 (14) (2016) 4063–4072, https://doi.org/10.1039/C6GC01028H.

[14] S. Keck, et al., Synthesis of a liquid Lignin-Based methacrylate resin and its application in 3D printing without any reactive diluents, Biomacromolecules 24 (4) (Apr. 2023) 1751–1762, https://doi.org/10.1021/acs.biomac.2c01505.

[15] L. Passauer, Highly swellable lignin hydrogels: novel materials with interesting properties, in: Functional Materials from Renewable Sources, in ACS Symposium Series, 1107, American Chemical Society, 2012, pp. 11–211, https://doi.org/10.1021/bk-2012-1107.ch011.

[16] L. Passauer, K. Fischer, F. Liebner, Preparation and physical characterization of strongly swellable oligo(oxyethylene) lignin hydrogels 65 (3) (2011) 309–317, https://doi.org/10.1515/hf.2011.044.

[17] L. Passauer, T. Hallas, E. Bäucker, G. Ciesielski, S. Lebioda, U. Hamer, Biodegradation of hydrogels from oxyethylated lignins in model soils, ACS Sustain. Chem. Eng. 3 (9) (Sep. 2015) 1955–1964, https://doi.org/10.1021/acssuschemeng.5b00139.

[18] I. Kühnel, B. Saake, R. Lehnen, A new environmentally friendly approach to Lignin-Based cyclic carbonates, Macromol. Chem. Phys. 219 (7) (2018) 1–6, https://doi.org/10.1002/macp.201700613.

[19] X. Wang, et al., Corrosion-resistant polyurethane coatings from structure-homogenized biorefinery lignin through fractionation and oxypropylation, J. Agric. Food Res. 10 (2022) 100452, https://doi.org/10.1016/j.jafr.2022.100452.

[20] L.-Y. Liu, S. Chen, L. Ji, S.-K. Jang, S. Renneckar, One-pot route to convert technical lignin into versatile lignin esters for tailored bioplastics and sustainable materials, Green. Chem. 23 (12) (2021) 4567–4579, https://doi.org/10.1039/D1GC01033F.

[21] Y. Xie, S. Gao, D. Zhang, C. Wang, F. Chu, Bio-based polymeric materials synthesized from renewable resources: a mini-review, Resour. Chem. Mater. 2 (3) (2023) 223–230, https://doi.org/10.1016/j.recm.2023.05.001.

[22] B. Atanasova, et al., Navigating process optimization in organosolv fractionation: a model-driven approach applied to poplar biomass, Sep. Purif. Technol. 377 (1) (2025) 134221, https://doi.org/10.1016/j.seppur.2025.134221.

[23] V. Mimini, et al., Lignosulfonate-based polyurethane materials via cyclic carbonates: preparation and characterization 74 (2) (2020) 203–211, https://doi.org/10.1515/hf-2018-0298.

[24] X. Meng, et al., Determination of hydroxyl groups in biorefinery resources via quantitative ^{31}P NMR spectroscopy, Nat. Protoc. 14 (9) (2019) 2627–2647, https://doi.org/10.1038/s41596-019-0191-1.

[25] D.S. Argyropoulos, N. Pajer, C. Crestini, Quantitative ^{31}P NMR analysis of lignins and tannins, JoVE (174) (2021) e62696, https://doi.org/10.3791/62696.

[26] I. Kühnel, B. Saake, R. Lehnen, Comparison of different cyclic organic carbonates in the oxyalkylation of various types of lignin, React. Funct. Polym. 120 (Nov. 2017) 83–91, https://doi.org/10.1016/j.reactfunctpolym.2017.09.011.

[27] E.A. Capanema, M.Y. Balakshin, J.F. Kadla, A comprehensive approach for quantitative lignin characterization by NMR spectroscopy, J. Agric. Food Chem. 52 (7) (Apr. 2004) 1850–1860, https://doi.org/10.1021/jf035282b.

[28] L.-Y. Liu, M. Cho, N. Sathitsuksanoh, S. Chowdhury, S. Renneckar, Uniform chemical functionality of technical lignin using ethylene carbonate for hydroxyethylation and subsequent greener esterification, ACS Sustain. Chem. Eng. 6 (9) (Sep. 2018) 12251–12260, https://doi.org/10.1021/acssuschemeng.8b02649.

[29] I. Kühnel, B. Saake, R. Lehnen, Oxyalkylation of lignin with propylene carbonate: influence of reaction parameters on the ensuing bio-based polyols, Ind. Crops Prod. 101 (Jul. 2017) 75–83, https://doi.org/10.1016/j.indcrop.2017.03.002.

[30] J. Lauwaert, et al., Pilot scale recovery of lignin from black liquor and advanced characterization of the final product, Sep. Purif. Technol. 221 (2019) 226–235, https://doi.org/10.1016/j.seppur.2019.03.081.

[31] K. Van Aelst, et al., Reductive catalytic fractionation of pine wood: elucidating and quantifying the molecular structures in the lignin oil, Chem. Sci. 11 (42) (2020) 11498–11508, https://doi.org/10.1039/D0SC04182C.

[32] A.T. Smit, T. Dezaire, L.A. Riddell, P.C.A. Bruijnincx, Reductive partial depolymerization of acetone organosolv lignin to tailor lignin molar mass, dispersity, and reactivity for polymer applications, ACS Sustain. Chem. Eng. 11 (15) (Apr. 2023) 6070–6080, https://doi.org/10.1021/acssuschemeng.3c00617.

[33] L. Krivdin, NMR studies of lignin and lignin-derived products: recent advances and perspectives, Russ. Chem. Rev. 94 (3) (2025) 1–28, https://doi.org/10.59761/RCR5159.

[34] C.A. Cateto, M.F. Barreiro, A.E. Rodrigues, M.C. Brochier-Salon, W. Thielemans, M. N. Belgacem, Lignins as macromonomers for polyurethane synthesis: a comparative study on hydroxyl group determination, J. Appl. Polym. Sci. 109 (5) (Sep. 2008) 3008–3017, https://doi.org/10.1002/app.28393.

[35] L. Ji, L.-Y. Liu, M. Cho, M.A. Karaaslan, S. Renneckar, Revisiting the molar mass and conformation of derivatized fractionated softwood kraft lignin, Biomacromolecules 23 (3) (Mar. 2022) 708–719, https://doi.org/10.1021/acs.biomac.1c01101.

[36] L.-Y. Liu, K. Bessler, S. Chen, M. Cho, Q. Hua, S. Renneckar, In-situ real-time monitoring of hydroxyethyl modification in obtaining uniform lignin derivatives, Eur. Polym. J. 142 (2021) 110082, https://doi.org/10.1016/j.eurpolymj.2020.110082.

[37] A. Duval, L. Avérous, Cyclic carbonates as safe and versatile etherifying reagents for the functionalization of lignins and tannins, ACS Sustain. Chem. Eng. 5 (8) (Aug. 2017) 7334–7343, https://doi.org/10.1021/acssuschemeng.7b01502.

[38] A. Duval, D. Vidal, A. Sarbu, W. René, L. Avérous, Scalable single-step synthesis of lignin-based liquid polyols with ethylene carbonate for polyurethane foams, Mater. Today Chem. 24 (2022) 100793, https://doi.org/10.1016/j.mtchem.2022.100793.

[39] A. Duval, G. Layrac, A. van Zomeren, A.T. Smit, E. Pollet, L. Avérous, Isolation of low dispersity fractions of acetone organosolv lignins to understand their reactivity: towards aromatic building blocks for polymers synthesis, ChemSusChem 14 (1) (Jan. 2021) 387–397, https://doi.org/10.1002/cssc.202001976.

[40] G. Galletti, et al., Glycerol carbonate as a versatile alkylating agent for the synthesis of β-Aryloxy alcohols, ACS Sustain. Chem. Eng. 10 (33) (Aug. 2022) 10922–10933, https://doi.org/10.1021/acssuschemeng.2c02795.

[41] J. Sternberg, O. Sequerth, S. Pilla, Valorizing depolymerized lignin oil through the Green synthesis of a thermoplastic non-isocyanate polyurethane, Polym. (Guildf.) 330 (2025) 128516, https://doi.org/10.1016/j.polymer.2025.128516.

[42] F.R. Vieira, A. Barros-Timmons, D.V. Evtuguin, P.C.R. Pinto, Effect of different catalysts on the oxyalkylation of eucalyptus Lignoboost® kraft lignin, Holzforschung 74 (6) (2020) 567–576, https://doi.org/10.1515/hf-2019-0274.

[43] D. Papp, G. Carlström, T. Nylander, M. Sandahl, C. Turner, A complementary multitechnique approach to assess the bias in molecular weight determination of lignin by Derivatization-Free gel permeation chromatography, Anal. Chem. 96 (26) (Jul. 2024) 10612–10619, https://doi.org/10.1021/acs.analchem.4c01187.

[44] Z. Li, E. Sutandar, T. Goihl, X. Zhang, X. Pan, Cleavage of ethers and demethylation of lignin in acidic concentrated lithium bromide (ACLB) solution, Green. Chem. 22 (22) (2020) 7989–8001, https://doi.org/10.1039/D0GC02581J.

[45] C.G. Yoo, et al., Understanding the physicochemical characteristics and the improved enzymatic saccharification of corn stover pretreated with aqueous and gaseous ammonia, BioEnergy Res. 9 (1) (2016) 67–76, https://doi.org/10.1007/s12155-015-9662-6.

[46] X. Duan, X. Wang, J. Chen, G. Liu, Y. Liu, Structural properties and antioxidation activities of lignins isolated from sequential two-step formosolv fractionation, RSC Adv. 12 (37) (2022) 24242–24251, https://doi.org/10.1039/D2RA02085H.

[47] L.-Y. Liu, Q. Hua, S. Renneckar, A simple route to synthesize esterified lignin derivatives, GREEN Chem. 21 (13) (Jul. 2019) 3682–3692, https://doi.org/10.1039/c9gc00844f.